

General phase diagram for antiferroelectric liquid crystals in dependence on enantiomeric excess

^{1,2}E. Gorecka, ¹D. Pociecha, ³M. Čepič, ³B. Žekš, ⁴R. Dabrowski

¹*Chemistry Department, Warsaw University, Al. Zwirki i Wigury 101, 02-089 Warsaw, Poland;*

²*Department of Microelectronics and Nanoscience, Chalmers University of Technology, S-41296 Göteborg, Sweden;*

³*J. Stefan Institute, Jamova 39, 1000 Ljubljana, Slovenia;*

⁴*Institute of Chemistry, Military University of Technology, 00-908 Warsaw, Poland.*

(December 15, 2021)

The phase diagram of the prototype antiferroelectric liquid crystal MHPOBC in dependence of enantiomeric excess was measured. It was shown that the Sm C_β^* phase in very pure samples is the Sm C_{FI2}^* phase with a four layer structure, and only after small racemization it transforms into the ferroelectric Sm C^* phase. The phase diagram was theoretically explained by taking into account longer range bilinear and short range biquadratic interlayer interactions, that lead to the distorted clock structures and first order transitions between them.

PACS numbers: 61.30.Cz

In some systems chiral properties can be transferred from a molecular to a macroscopic level. The best examples of such systems are liquid crystals which form chiral phases (cholesteric, blue, twist grain boundary or polar smectic phases), if built of chiral molecules. The variation of the enantiomeric excess influences macroscopic properties of these phases like the period of the modulation and the phase transition temperature or it can even change the phase sequence. The striking example of the last phenomenon are antiferroelectric liquid crystals where some phases disappear with racemization [1]. For high optical purity MHPOBC compound, the prototype antiferroelectric material, the sequence of tilted phases Sm $C_\alpha^* \leftrightarrow$ Sm $C_\beta^* \leftrightarrow$ Sm $C_\gamma^* \leftrightarrow$ Sm C_A^* was reported with decreasing temperature [2]. In the partially racemized sample only two of these phases, Sm C_β^* and Sm C_A^* , remained. The Sm C_A^* phase is the phase with the antiferroelectric properties and antiparallel tilts in neighboring layers, i.e., anticlinic phase. The Sm C_β^* phase has been recognized as the ferroelectric synclitic Sm C^* phase. Almost ten years later structures of the other subphases have been found by resonant x-ray scattering in a different compound (S-10OTBBB1M7) [3]. In this compound the phase sequence with decreasing temperature is: the Sm C_α^* phase with the periodical modulation of a tilt direction and with 5- or more, in general incommensurate, number of layers, the Sm C_{FI2}^* phase with 4-layer modulation, the Sm C_{FI1}^* phase with 3-layer modulation, and the Sm C_A^* phase with 2-layer structure. The Sm C_{FI1}^* phase in the 10OTBBB1M7 compound corresponds to the Sm C_γ^* phase in MHPOBC material. So far theoretical considerations failed to account for the correct phase sequences in dependence of enantiomeric excess as well as experimentally consistent structures of some phases.

In this Letter we present the complete phase diagram for the antiferroelectric system MHPOBC with respect to the enantiomeric excess. We show that the synclitic

Sm C^* phase transforms into the Sm C_{FI2}^* phase upon increasing optical purity. The result solves the long known controversy why the smectic Sm C_β^* phase in MHPOBC was first reported as a typical ferroelectric phase [2] and later also as the phase having antiferroelectric properties [4]. We show here, that this system is a nice example of intermediate phases, which appear between main phases because of the cancelation of short range interactions and consecutive relevance of small chiral and/or longer range interactions. We present a new phenomenological model, which takes into account longer range bilinear [5] and short range biquadratic [6] interlayer interactions and allows for correct enantiomeric excess dependent phase sequence with first order transitions between experimentally consistent structures.

Several S-enantiomer rich [7] mixtures of MHPOBC were studied by differential scanning calorimetry (DSC), dielectric and optical methods. The DSC measurements were performed using Perkin Elmer DSC-7 calorimeter in the cooling and heating runs at scanning rates 0.2-1 K/min. In the dielectric measurements the glass cells of various thickness, with 25 mm² ITO electrodes coated by polyimide, were used. Dielectric spectroscopy studies were performed with HP 4192A impedance analyzer. In each phase the dielectric spectra were fitted with Cole-Cole equation. The selective reflection measurements were performed in transmission mode at normal incidence (Shimadzu 3101PC spectrophotometer) for one surface free (made on the quartz plate) or film samples. These studies allowed to determine the helical pitch in Sm C_A^* and Sm C^* phases.

In the Sm C_{FI1}^* and Sm C_{FI2}^* phases the pitch was estimated by the direct microscopic observations of periodicity of the line defects in 40 micron homogeneously aligned cell. The thick (250 micron) film samples were used for the optical rotatory power (ORP) measurements, in which a standard setup was used where the analyzer is rotated against the polarizer to obtain a minimum of the light (630 nm) transmission.

In the optically pure samples (enantiomeric excess $x = c_S - c_R = \pm 1$ where c_S and c_R are corresponding concentrations) four tilted smectic subphases with historical names $\text{Sm } C_\alpha^*$, $\text{Sm } C_\beta^*$, $\text{Sm } C_\gamma^*$, $\text{Sm } C_A^*$ appear below the $\text{Sm } A$ phase (Fig. 1). Two phases which appear between the $\text{Sm } C_\alpha^*$ and $\text{Sm } C_A^*$ phase, have rather long helical pitch. The periodicity of disclination lines which could be observed in the thick planar cell, is about $2.5 \mu\text{m}$ in higher temperature phase (denoted as $\text{Sm } C_\beta^*$) and about $1.6 \mu\text{m}$ in the lower temperature phase (denoted as $\text{Sm } C_\gamma^*$). No selective reflection in a visible range, which is encountered in the lower purity MHPOBC materials, could be detected at any temperature. Both intermediate phases have a pronounced optical activity, $+35^\circ/\mu\text{m}$ and $-10^\circ/\mu\text{m}$ in $\text{Sm } C_\gamma^*$ and $\text{Sm } C_\beta^*$, respectively, that is only slightly temperature dependent in the each phase temperature interval. Except for the temperature region of $\text{Sm } C_\beta^*$, the results of ORP measurements agree with those presented in [8]. Dielectric spectroscopy measurements clearly exclude the presence of the ferroelectric synclinic $\text{Sm } C^*$ phase (Fig. 2a). In the $\text{Sm } A$ phase, single, high frequency relaxation process is observed that softens, e.g. the mode frequency decreases and its amplitude increases, when approaching the $\text{Sm } C_\alpha^*$ phase. In the $\text{Sm } C_\alpha^*$ phase a single mode at $\sim 60 \text{ kHz}$ was observed. In the $\text{Sm } C_\beta^*$ phase weak ($\Delta\epsilon \sim 4$), high frequency (350kHz) mode was detected, typical for the phase with an antiferroelectric order. Similarly as in the $\text{Sm } C_A^*$ phase [9] this mode is either related to the distortion of the crystallographic unit cell or to the rotation of the molecules around their main axes. Absence of the Goldstone mode excludes that $\text{Sm } C_\beta^*$ phase is the ferroelectric $\text{Sm } C^*$ phase.

Dielectric permittivity increases upon entering the $\text{Sm } C_\gamma^*$ phase. Here the main contribution to the dielectric susceptibility comes from the low frequency relaxation process at 1-2 kHz, sometimes called the ferroelectric Goldstone mode [10]. The relaxation frequency of the mode detected in the $\text{Sm } C_\gamma^*$ phase is not well defined. The parameter α in the Cole-Cole formula, that characterizes the distribution of the relaxation frequencies, is about 0.3. The presence of a broad mode is inherent to the $\text{Sm } C_\gamma^*$ phase. The dielectric permittivity again decreases in the $\text{Sm } C_A^*$ phase, in this phase two weak modes ($\Delta\epsilon < 1$) could be seen in MHz frequency region. Above results show that the $\text{Sm } C_\gamma^*$ phase is the ferroelectric phase identical as the $\text{Sm } C_{FI1}^*$ and the $\text{Sm } C_\beta^*$ phase is the antiferroelectric phase, biaxial thus optically active and distinctly different than the $\text{Sm } C_A^*$ phase. Thus we conclude that the $\text{Sm } C_\beta^*$ phase has the distorted clock four-layer structure of the $\text{Sm } C_{FI2}^*$ phase.

In the samples with a slightly lower optical purity ($x \sim 0.97$) five subphases could be identified below $\text{Sm } A$ phase from the DSC thermograms (Fig.1) and microscopic studies. An additional phase, which appears between the $\text{Sm } C_\alpha^*$ and the $\text{Sm } C_{FI2}^*$ phases, gives selec-

tive reflection in the visible light range. Selective reflection wavelength changes from 450 nm to 600 nm within the phase temperature interval. Since the temperature range of the $\text{Sm } C_{FI2}^*$ phase in this mixture is rather narrow it is difficult to observe all five phases in the dielectric measurements. Due to the small temperature gradients that are hard to avoid in the sample with the big electrode area, the $\text{Sm } C_{FI2}^*$ phase always coexists with the additional phase. In this additional phase the dielectric permittivity is an order of magnitude stronger than in all other phases (Fig.2b) thus typical for the synclinic ferroelectric $\text{Sm } C^*$ phase.

As the optical purity decreases further, the $\text{Sm } C_{FI2}^*$ phase disappears and in the excess range between 0.88-0.97 the phase sequence $\text{Sm } C_\alpha^* \leftrightarrow \text{Sm } C^* \leftrightarrow \text{Sm } C_{FI1}^* \leftrightarrow \text{Sm } C_A^*$ is observed, that is the phase sequence incorrectly reported in literature for the pure enantiomeric MHPOBC compound [2]. In mixtures with $x < 0.88$ also $\text{Sm } C_{FI1}$ is missing. As the enantiomeric excess is further reduced ($x < 0.5$), finally the $\text{Sm } C_\alpha^*$ disappears, and only $\text{Sm } A$, $\text{Sm } C^*$ and $\text{Sm } C_A^*$ phases are left. Based on above observations the phase diagram in dependence on enantiomeric excess as shown in Fig. 3 is proposed. We believe that this type of the phase diagram is general for antiferroelectric liquid crystals.

To account for experimental observations theoretically, we introduce a new phenomenological model with bilinear interlayer interactions between the tilt vectors ξ_j which are of longer range [5], and with biquadratic quadrupolar NN interactions [6], which become more important at larger tilts i.e. at lower temperatures. The interlayer part of the free energy is

$$G_{int} = \frac{1}{2} \sum_j \left(\sum_{i=1}^4 \tilde{a}_i (\xi_j \cdot \xi_{j+i}) + \sum_{i=1}^3 \tilde{f}_i (\xi_j \times \xi_{j+i}) + b_Q (\xi_j \cdot \xi_{j+1})^2 \right). \quad (1)$$

Achiral parameters \tilde{a}_i and chiral parameters \tilde{f}_i depend on steric and on van der Waals interactions to nearest neighboring layers (NN), on electrostatic interactions to NN and next nearest neighboring layers (NNN), on intralayer chiral piezoelectric and NN flexoelectric coupling. They are given by Eq.(6) in the Ref. [5]. We assume that for the racemic mixture parameter \tilde{a}_1 is negative favoring synclinic tilts at higher temperatures and becomes positive favoring anticlinic tilts at lower temperatures. In chiral samples it gains additional positive contribution proportional to x^2 , thus changes the sign at higher temperature. Parameter \tilde{a}_2 is positive and does not depend on the enantiomeric excess considerably. Quadrupolar NN interactions b_Q are excess independent. All parameters are expressed in degree Kelvin [5].

Numerical analysis of the above model gives the phase diagrams which are in qualitative agreement with the experimentally obtained one Fig. 3. This detailed anal-

ysis will be published elsewhere and here only the basic physical understanding is given. In racemic mixtures the synclinal negative \tilde{a}_1 term prevails over the anticlinical positive \tilde{a}_2 term directly below the transition from the Sm A to the tilted phase and the Sm C* phase appears. Upon decreasing temperature, \tilde{a}_1 increases and changes its sign at a temperature where quadrupolar term is already significant. Since this term favors both synclinal and anticlinical tilts in NN layers, direct transition from the Sm C* phase to the Sm C_A* phases is obtained. In chiral samples, the anticlinical part of the parameter \tilde{a}_1 increases and \tilde{a}_1 becomes by its absolute value comparable to the parameter \tilde{a}_2 directly below the transition to the tilted phase. This results in a formation of the Sm C_α* phase with the short pitch modulation which becomes stable over a wider temperature range upon increasing enantiomeric excess. It evolves into the Sm C* phase due to increasing quadrupolar interactions. Due to increased enantiomeric excess also the temperature increases where the \tilde{a}_1 changes sign. Therefore the influence of quadrupolar interactions is weaker and cannot prevent the existence of modulated phases. With purification also the temperature range of modulated phases increases. In the temperature region where $\tilde{a}_1 \approx 0$ the structure with two interchanging phase differences α and β with $\alpha + \beta \approx \pi$, is formed. The quadrupolar term b_Q favors values of $\alpha = 0$ and $\beta = \pi$ but chiral NN interactions increase the value of α and decrease the value of β . This structure obtained by the minimization of the Eq. (1) is consistent with a tentatively proposed structure for the Sm C_{FI2}* phase [11,12]. The structure has the biaxial unit cell, a negligible polarization and is helicoidally modulated with the long optical pitch defined by δ (Fig.4a). Decreasing the temperature further, the parameter \tilde{a}_1 becomes positive and thus simultaneously with the \tilde{a}_3 parameter encourages the structure where tilts in third neighboring layers are synclinal. Due to the up down symmetry, the phase difference α is followed by two equal phase differences β where $\alpha + 2\beta \approx 2\pi$. The obtained unit cell is polar and biaxial. The structure is helicoidally modulated with the long optical pitch defined by δ (Fig. 4b). It can be recognized as the one proposed for the Sm C_{FI1}* phase [11,12]. In pure samples the temperature range of the Sm C_α* phase and the temperature range of the modulated phases are so wide that the Sm C* phase cannot evolve and direct phase transition between the Sm C_α* phase and the Sm C_{FI2}* phase occurs as observed in MHPOBC.

To conclude, in this Letter we report experimental and theoretical studies which show that in the optically pure antiferroelectric liquid crystal MHPOBC, the Sm C_β* phase is not the ferroelectric Sm C* phase but the Sm C_{FI2}* phase with four-layer unit cell and antiferroelectric properties. The ferroelectric Sm C* phase appears only after a slight racemization. For antiferroelectric liquid crystals the general phase diagram with respect to

enantiomeric excess is proposed. We also proposed the new free energy for polar smectics which includes achiral and chiral bilinear interlayer interactions to more distant layers and quadrupolar NN interactions. This free energy allows for the correct enantiomeric excess dependent phase sequence as well as the experimentally consistent structures of all phases and first order transitions between them.

Acknowledgment: This work was supported by Polish-Slovenian exchange program. The financial support for E.G. from *TFR* Swedish Research Council is acknowledged. E.G. is grateful to Prof. S. Lagerwall for his hospitality during her stay at the Chalmers University.

-
- [1] A.Fukuda, Y.Takanishi, T.Isozaki, K.Ishikawa and H.Takezoe, *J.Mat.Chem.* **4**, 997 (1994).
 - [2] A.D.L.Chandani, E.Gorecka, Y.Ouchi, H.Takezoe and A.Fukuda *Jap.J.App.Phys.* **28**, L1265, (1989); E.Gorecka, A.D.L.Chandani, Y.Ouchi, H.Takezoe and A.Fukuda, *Jap.J.Appl.Phys.* **29**, 131 (1990).
 - [3] P.Mach, R.Pindak, A.-M.Levelut, P.Barois, H.T.Nguyen, C.C.Huang, and L.Furenid, *Phys. Rev. Lett.* **81**, 1015 (1998). P.Mach, R.Pindak, A.-M.Levelut, P.Barois, H. T.Nguyen, H.Baltes, M.Hird, K.Toyne, A.Seed, J.W.Goodby, C.C.Huang, and L.Furenid, *Phys.Rev.E* **60**,6793, (1999).
 - [4] J.F.Li, E.A.Shack, Y.K.Yu, X.Y.Wang, C.Rosenblatt, M.E. Neubert, S.S.Keats and H.Gleeson *Jap. J.Appl.Phys.* **2 35**, L1608 (1996); T.Sako,Y.Kimura, R.Hoyakawa, N.Okabe, Y.Suzuki, *Jap.J.Appl.Phys.* **235**, L114 (1996); A. Jakli *J.Appl.Phys.* **85**, 1101 (1999).
 - [5] M.Čepič, B.Žekš, *Phys.Rev.Lett* **87**, 085501 (2001).
 - [6] D.Pociecha, E.Gorecka, M.Čepič, N.Vaupotič, B.Žekš, D.Kardas, and J.Mieczkowski, *Phys.Rev.Lett.* **86**, 3048 (2001).
 - [7] R- or S- octanol-2 with 99.5% enantiomeric excess was used for the synthesis of the MHPOBC compound as described by W.J. Drzewinski Phd thesis, (2000).
 - [8] M.Škarabot, M.Čepič, B.Žekš, R.Blinc, G.Heppke, A.V.Kityk, I.Mušević, *Phys.Rev.E* **58**, 575 (1998)
 - [9] Yu.P.Panarin, O.Kalinovskaya, J. K.Vij, J.W.Goodby *Phys.Rev.E* **55**, 4345 (1997).
 - [10] S.Merino, M.R.de la Fuente, Y.González, M.A.Pérez Jubindo, B.Ros, J.A.Puértolas, *Phys.Rev.E* **54**, 5169 (1996); M.Čepič, G.Heppke, J.M.Hollidt, D.Lötzsch, B.Žekš, *Ferroelectrics* **147**, 43 (1993); M.Glogarova, H.Sverenyuk, H.T.Nguyen, C.Destrade, *Ferroelectrics* **147**, 159 (1993).
 - [11] T.Akizuki, K.Miyachi, Y.Takanishi, K.Ishikawa, H.Takezoe and A.Fukuda, *Jpn.J.Appl.Phys.* **38**, 4832(1999).
 - [12] P.M.Johnson, D.A.Olson, S.Pankratz, T.Nguyen, J.Goodby, M.Hird and C.C.Huang, *Phys.Rev.Lett.* **84**, 4870 (2000).

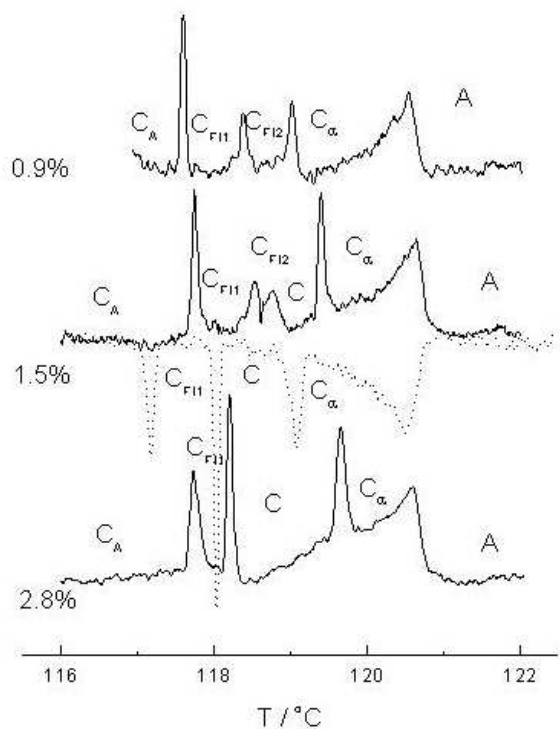


FIG. 1. DSC scans for MHPOBC mixtures with various percentage of R enantiomer measured in heating scans with 1 K/min rate. For concentration 1.5% the cooling scan is also shown.

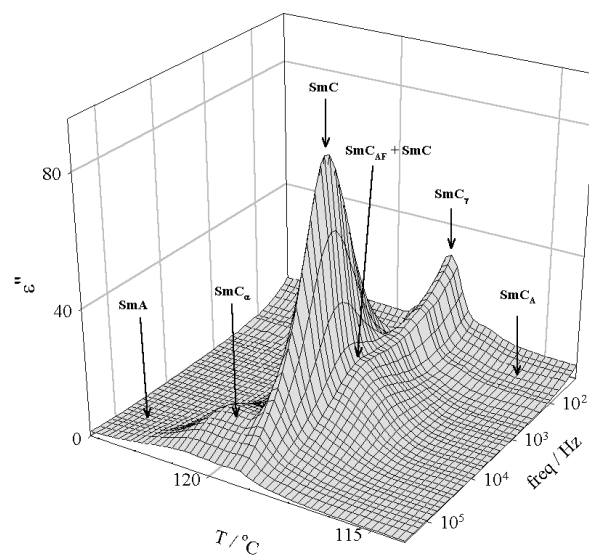
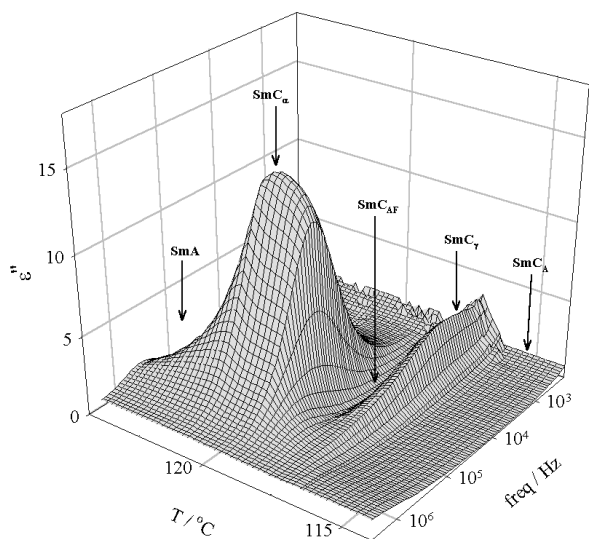


FIG. 2. Dielectric losses vs. temperature and frequency in S-MHPOBC enantiomer (a) and and its mixture with 1,5% of R-enantiomer (b).

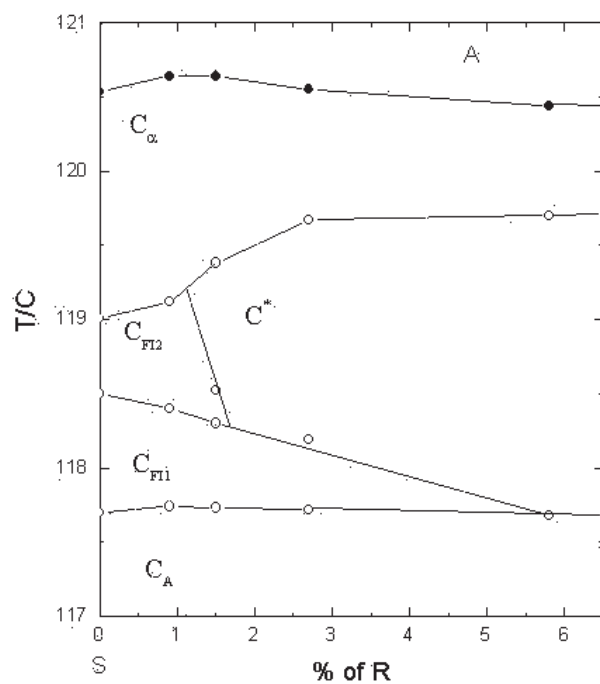


FIG. 3. Phase diagram for MHPOBC in dependence of optical purity.

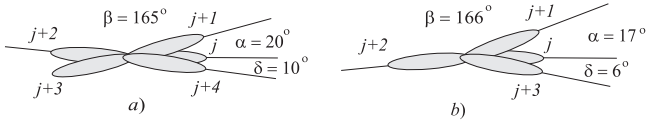


FIG. 4. a) The Sm C_{FI2}^* phase and b) the Sm C_{FI1} phase obtained for the optically pure material $x = 1$ and the set of parameters expressed in K (Eq.(6), Ref.[5]): $a_1 = (-4.1 + 90 \theta^2)$, $c_p = 0.6$, $\mu = 0.77$, $b_0 = 2$, $b_1 = b_0/5$, $b_2 = b_0/100$, $f_1 = 0$ and for $b_Q = -17.7$. Corresponding set of effective parameters expressed in mK is: $\tilde{a}_2 = 73.5$, $\tilde{a}_3 = -7.41$, $\tilde{a}_4 = 0.65$, $\tilde{f}_1 = -231$, $\tilde{f}_2 = 23.1$ and $\tilde{f}_3 = 2.02$. The tilt angle is taken from Ref.[8] for (a) $\theta = 12.5^\circ$ and therefore $\tilde{a}_1 = 137$ mK and for (b) $\theta = 13.2^\circ$ and $\tilde{a}_1 = -69.6$ mK.